

Study of the design of CSNS MEBT

OUYANG Hua-Fu(欧阳华甫) LIU Hua-Chang(刘华昌) FU Shi-Nian (傅世年)

(Institute of High Energy Physics, CAS, Beijing 100049, China)

Abstract The design of CSNS MEBT has two objectives: (1) to match the beam both in the transversal direction and the longitudinal direction from RFQ into DTL; (2) to further chop the beam into the required time structure asked by RCS. It is very difficult and critical to control well the emittance growth and in the meantime to match and chop the beam. Firstly, the optical design is done and optimized, and the multi-particle simulations show that the maximum emittance growth is successfully controlled within 14%. Secondly, based on the different beam envelopes obtained by TRACE-3D and PARMELA, the least deflecting angle of the chopper is determined by TRACE-3D. At last, the field of steering magnet is determined through simulations.

Key words MEBT, chopper, match, beam envelope, emittance growth, central orbit

PACS 41.85.Ja, 41.85.Ew, 29.20.Ej

1 Introduction

The China Spallation Neutron Source (CSNS) is an accelerator-based high power project currently under R&D in China^[1, 2]. The accelerator complex consists of an 81 MeV H^- linear accelerator as the injector and a 1.6 GeV rapid cycling proton synchrotron (RCS). The linear accelerator consists of a 50 keV H^- Penning surface plasma ion source, a low beam energy transport line (LEBT), a 3.0 MeV radio frequency quadrupole (RFQ) accelerator, a medium energy beam transport line (MEBT), an 81 MeV drift tube linear accelerator (DTL) and a high energy beam transport line (HEBT). MEBT is located between RFQ and DTL, and one of its main functions is to match the beam from RFQ into DTL both in the two transversal directions and the longitudinal direction. To realize well the beam matching, the necessary beam diagnostic components are also arranged in MEBT. In order to decrease the beam loss during the beam injection process from the linac to the rapid cycling synchrotron (RCS), a pre-chopper is arranged in LEBT to pre-chop the beam from ion source into the required beam time structure asked by RCS. For CSNS Phase-I, a 20 mA pulsed beam extracted from the ion source is enough to satisfy the average beam power of 100 kW needed for the accelerator complex. However, a beam with a pulsed current of 40 mA is required for the upgrade of CSNS in the future (CSNS

Phase-II). For CSNS Phase-II, a chopper will be arranged in MEBT to further sharpen the beam edges kept by the pre-chopper during its rising time and falling time. The design of MEBT is carried out with the chopper taken into account although the chopper will not be used for CSNS Phase-I.

The physics design of the MEBT is tightly constrained by the requirement that the emittance growth should be held to a value as low as possible. To control the emittance growth (it is generally desired to control the emittance growth under 20%), which is mainly caused by the nonlinear space charge force, MEBT should be designed as short as possible. For example, the MEBT length is about 3640 mm^[3] for the Spallation Neutron Source (SNS) in USA, and is 3008.5 mm^[4] for the Japan Proton Accelerator Research Complex (J-PARC). The filament of the beam in the bunchers can also lead to nonlinear space charge force and therefore is another important factor to enhance the emittance growth. The buncher is a component to match the beam in the longitudinal direction. The focusing lattice being as regular as possible can largely limit the nonlinear space charge distribution and therefore weaken the emittance growth too.

2 Optical design

As mentioned in the introduction, in order to

Received 28 September 2008

©2009 Chinese Physical Society and the Institute of High Energy Physics of the Chinese Academy of Sciences and the Institute of Modern Physics of the Chinese Academy of Sciences and IOP Publishing Ltd

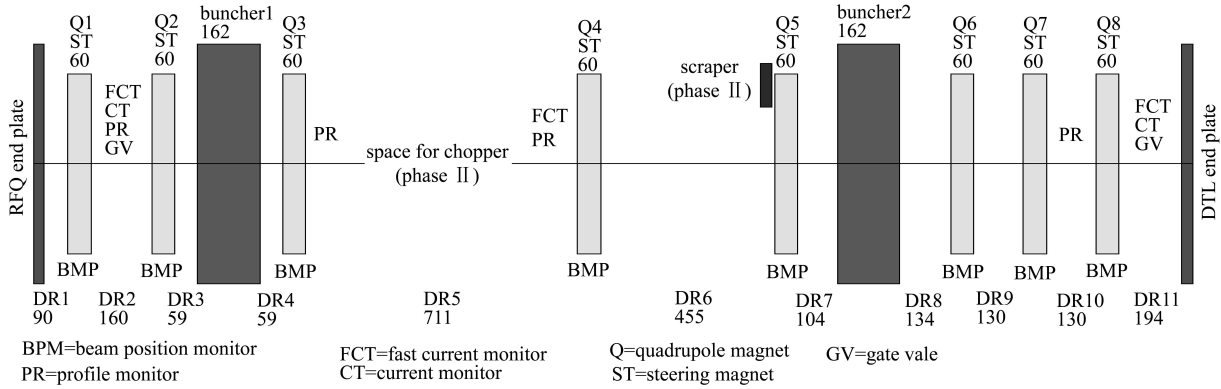


Fig. 1. The schematic drawing of CSNS MEBT.

satisfy the CSNS Phase-II requirement on a pulsed beam current of 40 mA, MEBT with a chopper is designed. Fig. 1 shows the schematic layout of the CSNS MEBT, which is structurally similar to J-PARC MEBT due to the same exit energy of RFQ and the similar DTL structure with J-PARC^[4]. It mainly consists of 8 quadrupoles, 2 bunchers and 1 chopper. In addition, two vacuum gate valves (GV) and a number of beam diagnostic components such as the beam position monitor (BPM), the current monitor (CT), the fast current monitor (FCT) and the profile monitor (PR) are also installed between or in the quadrupoles. 8 sets of steering magnets are incorporated into quadrupoles through wiring on the quadrupole yokes. A 711 mm long space is left to accommodate the chopper, and the first 4 quadrupoles are arranged to serve for the chopper. The chopper under design could be of a traveling wave or a standing wave structure^[5, 6]. Table 1 lists the design values of 8 quadrupoles and two bunchers both for the currents of 20 mA and 40 mA. From Table 1 one can see that the variation of the design values of the quadrupole and the buncher is very small when the beam current changes from 20 mA to 40 mA.

Table 1. Parameter values for quadrupoles and bunchers both in the cases of currents of 20 mA and 40 mA.

elements	(gradient/(T/m))/(gap-voltage/MV)		length/mm
	20 mA	40 mA	
Q1	-30	-33	60
Q2	26	27	60
Buncher1	0.106	0.124	162
Q3	-16	-17.5	60
Q4	12	12	60
Q5	-14.1	-13.8	60
Buncher2	0.140	0.148	162
Q6	21.2	20.2	60
Q7	-23.2	-24.6	60
Q8	12.2	16.5	60

Figure 2 shows the 6 times the rms (6σ) beam envelope and phase spread in MEBT obtained by code TRACE-3D^[7]. Here a 6σ beam envelope instead of a common 5σ is used. The reason is that all RFQ design codes and multi-particle simulation codes use 6σ , and the RFQ multi-particle simulation results obtained by code PARMTEQM show that, only 97.3% of particles are included in the 6σ beam envelope at the exit of RFQ. The maximum envelopes both in the horizontal direction and in the vertical direction are about 8.5 mm, which locates at the centers of the fifth and the second quadrupoles, respectively. The maximum envelope in the longitudinal direction occurred at the center of the second buncher, which is about 54° . The chopped beam will be deflected out horizontally and separated completely from the un-chopped beam at the scraper, which just locates at the front of the fifth quadrupole. The chopped beam bombards on the scraper, and the chopped beam power is brought out from the scraper by the cooling water. To make the beam bore of the chopper as small as possible, the first 3 quadrupoles are used to ensure a small horizontal envelope at the exit of the chopper, where the beam has already had a certain amount of offset from the beam axis due to deflection of the chopper. To lower the deflecting angle of the beam produced by the chopper, the fourth quadrupole is used as an amplifier to further enlarge the chopped beam deviation from the axis at the scraper. Although the beam envelope is also enlarged at the same time, the enlarging degree of the envelope is less than that of the deviation, for the chopped beam deviation is larger than the beam envelope at the fourth quadrupole as will be shown later. In the meantime, a comparative large beam envelope is beneficial to the cooling of the scraper. The last four quadrupoles and two bunchers are adopted to match the beam from RFQ into DTL in the two transversal directions and the longitudinal direction, respectively. Though theoretically one

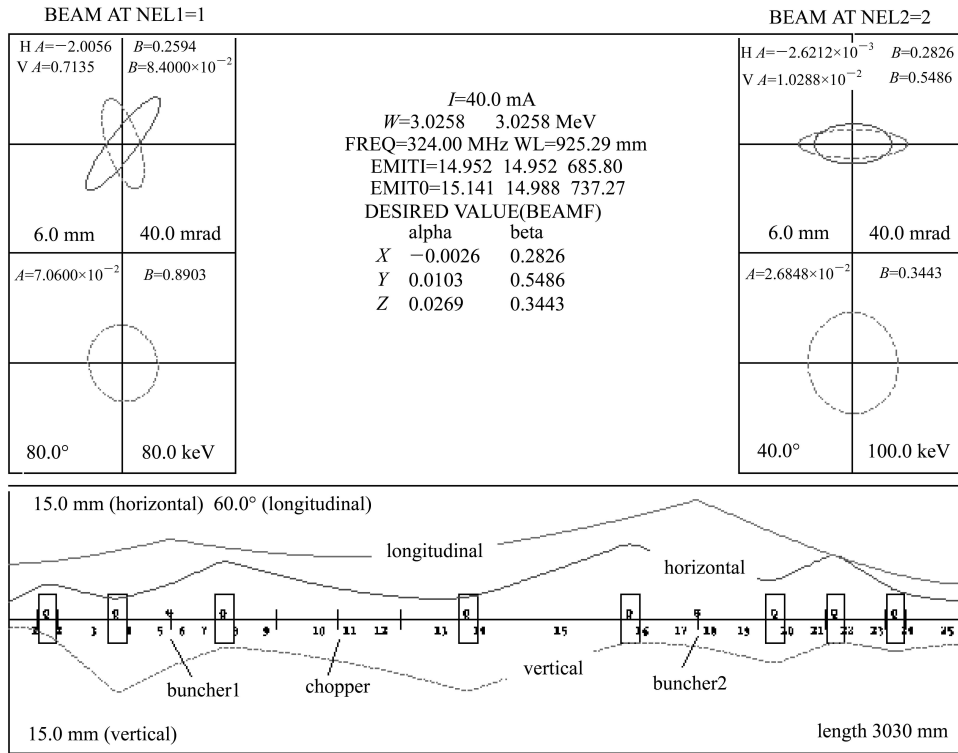


Fig. 2. 6σ beam envelope and phase spread in MEBT.

buncher can match the beam longitudinally, here two bunchers are still used to decrease the beam filament extent and therefore the emittance growth. For instance, four bunchers are used in MEBT for SNS and two bunchers for J-PARC.

3 Multi-particle simulations

The TRACE-3D code treats the particle distribution as a homogeneous distribution in an ellipse of phase space, and the space charge force is treated as a linear force. The emittance does not grow in the beam transporting process except in the buncher. In the buncher, the beam filament caused by the nonlinear RF electric force can give rise to the emittance growth, especially the emittance growth in the z direction. As shown in Fig. 2, the total emittance growth due to the two bunchers is about 1.26%, 0.24%, 7.5% in the x , y and z directions, respectively. However, in practice, the particle is generally not homogeneously distributed and the space charge force is also nonlinear. To reflect the beam transportation in MEBT more precisely and practically, multi-particle simulations are carried out by code PARMELA. PARMELA can include a 3-dimension (3-D) space-charge calculation that uses an adaptation of the fast 3-D particle-in-cell (PIC) routine written by Robert Ryne^[8]. The multi-particle tracking simulations of MEBT are started from the exit

of RFQ and the initial beam particle distribution tracked by PARMILA is output by the RFQ multi-particle tracking code PARMTEQM. The left part of Fig. 3 shows the initial beam particle distribution in the x - y plane at the exit of RFQ output by PARMTEQM and the right part of Fig. 3 shows the last particle distribution in the x - y plane at the exit of MEBT output by PARMELA. Since the simulated macro particle number is 100000 at the entrance of RFQ by PARMTEQM, the actual tracking particle number by PARMELA is only near to 100000 because the beam transmission in RFQ is about 97%. Fig. 4 shows the beam envelopes at the element positions. From Fig. 4 one can see that the maximum envelope locates at the center of the fifth quadrupole. This envelope obtained by PARMELA is about 1.25 times larger than the 6σ beam envelope at the same position obtained by TRACE-3D. Due to the nonlinear space charge force, the emittance growth obtained by PARMELA is also different from that obtained by TRACE-3D. As shown in Fig. 5, the maximum rms emittance growth is about 14%, which occurs in the x direction, and the value is also much larger than the emittance growth of 1.26% obtained by TRACE-3D. The rms emittance growth obtained by PARMELA in the y and z directions is 4.5% and 1.1%, respectively, which is also different from that obtained by TRACE-3D. The emittance growth in the y direction obtained by PARMELA is larger than that obtained

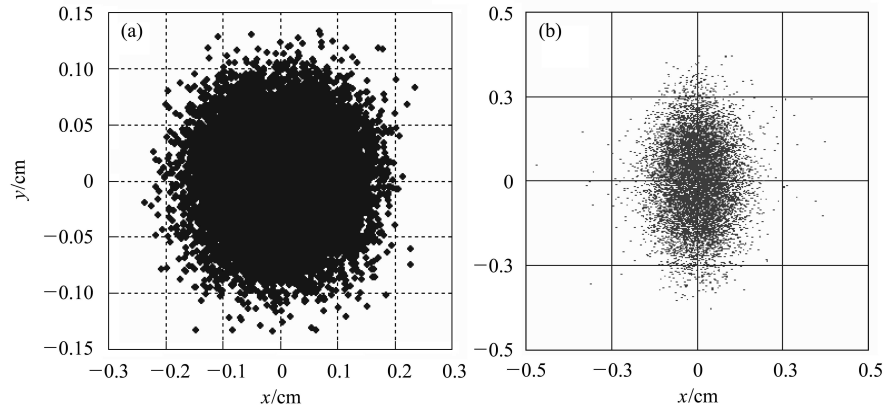


Fig. 3. The beam particle distributions: (a) the initial distribution at the exit of RFQ output by PARMTEQM; (b) the last particle distribution at the exit of MEBT obtained by PARMELA.

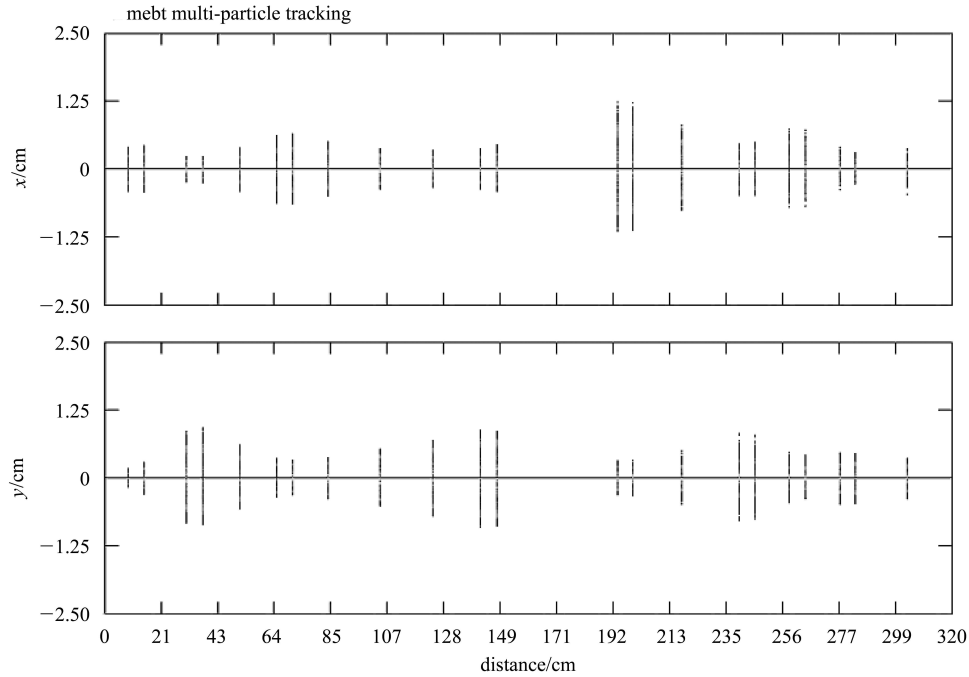


Fig. 4. The beam envelopes at the element positions obtained by code PARMELA.

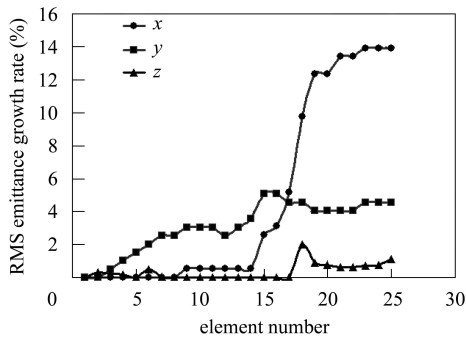


Fig. 5. The rms emittance growth in the x (dot), y (square) and z (triangle) directions versus the element obtained by the code PARMELA.

by TRACE-3D, but the emittance in the z direction obtained by PARMELA is smaller than that obtained

by TRACE-3D. The maximum rms emittance growth of CSNS MEBT is lower than that of J-APARC and SNS MEBT^[3, 4]. From Fig. 5 one can see that the emittance growth in the x direction mainly occurs in the beam transporting process from the fourth quadrupole to the second buncher. One of the main reasons for the quick emittance growth in the x direction should be the strong nonlinear space charge force due to the very small beam envelope in the x direction from the chopper to the fourth quadrupole.

Here the code PARMELA is used to do a multi-particle simulation. PARMELA and IMPACT are the other two codes that are often used to do multi-particle simulations for the transport line or the linear accelerator. But since the three codes use the same 3-dimension PIC routine to calculate the space

charge force, the results obtained by these codes are not essentially different.

4 The least chopping angle

As mentioned above, the chopper under design will be a traveling-wave mode cavity or a standing-wave mode cavity and the detailed design will be not given here. Before designing the chopper, it is necessary to firstly determine the least deflecting angle of the chopper with which the chopped beam will just separate from the un-chopped beam completely at the location of the beam scraper. The practical design deflection angle of the chopper can then be obtained by adding a certain amount of safety margin on the basis of the least deflecting angle. However, since the beam envelope obtained by TRACE-3D is largely different from that obtained by PARMELA, the least deflecting angles of the chopper obtained based on the different beam envelopes must also be different.

Although there is not a chopper element for the

code TRACE-3D, one can still easily track the deflecting beam and get the needed deflecting angle with a neglecting error by using the element of “quadrupole” in code TRACE-3D. The chopper function of the element of “quadrupole” is realized by setting B' (magnetic-field gradient) as a small value, l (effective length) the same as the length of the chopper, and dx (offset in x) as a large value. Fig. 6 shows the chopped beam center trajectory in the x direction after deflecting by the ‘chopper’. From the figure one can see that, at the location of the scraper, the distance (17.0 mm) of the chopped beam center from the beam axis is just two times the beam envelope (8.5 mm) obtained by TRACE-3D. The least deflecting angle calculated at the exit of the chopper is 11.33 mrad. The least deflecting angle obtained above is based on the beam envelope of 8.5 mm obtained by TRACE-3D. Using the same method, one can get the least deflecting angle at the exit of the chopper based on the beam envelope obtained by PARMELA, which is about 14.22 mrad.

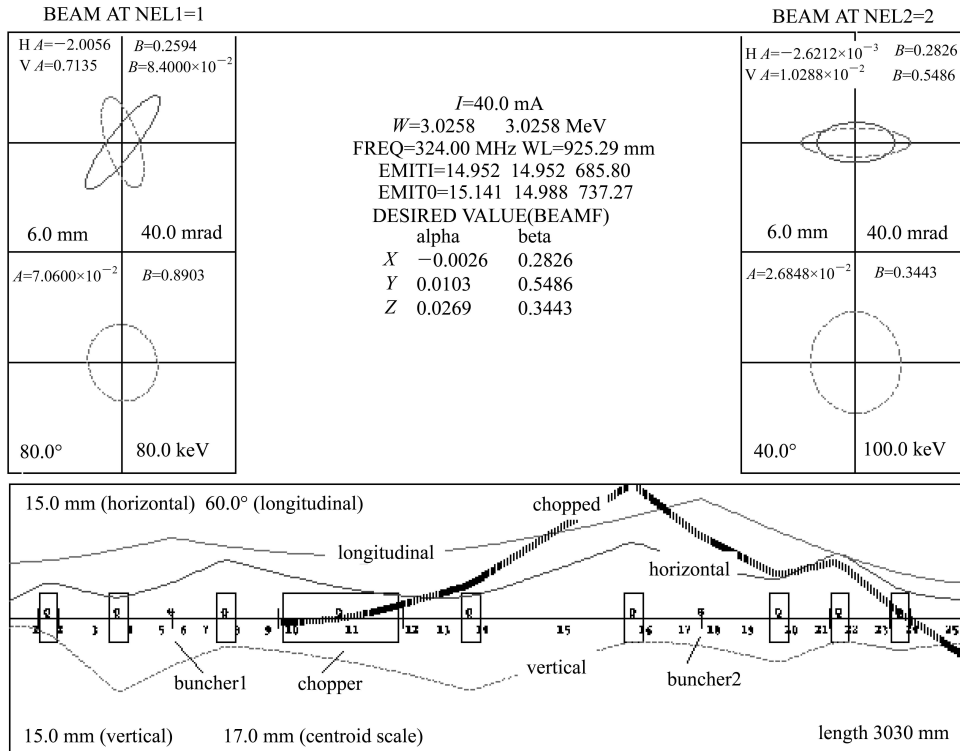


Fig. 6. The trajectory of the chopped beam center in the x direction.

5 Design of the buncher

The longitudinal length and accelerating voltage of the buncher have been given in the optical design, as listed in Table 1. The beam aperture of the

buncher can also be determined based on the beam envelope (given by TRACE-3D or PARMELA) at the location of the buncher. Although the voltage and beam aperture requirements of the two bunchers are different, the same geometry is still chosen for simplicity and economy of buncher manufacture. The nose-

cone CCL type structure is adopted for its simplicity, higher impedance and lower risk of multipacting compared with other cavity types, such as the quarter-wave cavity and the pill-box with quadrupoles inside nose-cones^[9]. The detailed design has been given in Ref. [9], and the main parameters of the buncher are listed in Table 2.

Table 2. Main parameters of the buncher.

beam kinetic energy/MeV	3.026
RF frequency/MHz	323.5
beam aperture diameter/mm	32
longitudinal length/mm	162
inner cavity diameter/mm	569
nose-cones separation/mm	15
Q value (computed)	27915.2
transit time factor	0.596
shunt impedance/ $M\Omega$ (linac convention)	2.28
$(R/Q)/\Omega$	40.964
nominal voltage/kV	156
peak dissipated power/kW	11.53
duty cycle	1.30%
peak electric field on nose cones/(MV/m)	26.107
ratio peak field to Kilpatrick limit	1.47

6 Field of the steering magnet

As mentioned in the introduction, the length of MEBT is designed to be as short as possible to control the beam emittance growth. To this end, 8 sets of steering magnets are incorporated into quadrupoles through wiring on the quadrupole yokes. But side effects are consequently also produced. If the field of the steering magnet is too strong, it will largely deteriorate the field distribution quality of the quadrupoles. On the contrary, if the field of this steering magnet is too weak, the distortion of the central orbit caused by the collimation tolerance, manufacturing error, etc. could not be easily corrected. To determine the maximum field of the steering magnets and therefore the corresponding magnet power supply parameters, simulations are done to seek the relation between the field of the steering magnet and the errors or the central orbit distortion. At last, the maximum field of the steering magnet is limited as 1/15 of the maximum field of the corresponding quadrupole. In this case, up to 14 mm deviation from the beam axis for the central orbit can be corrected through the steering magnets, as shown in Fig. 7.

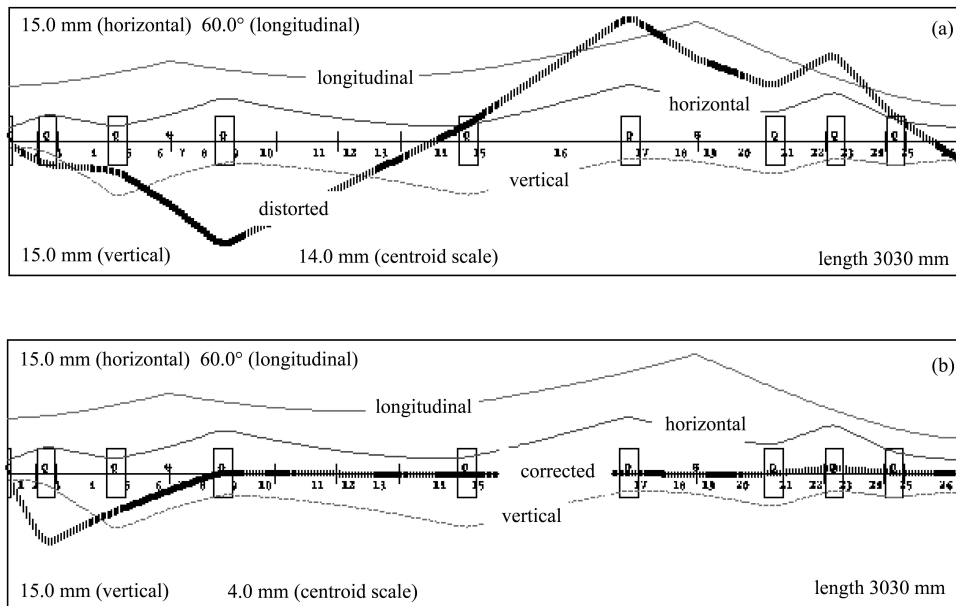


Fig. 7. The distorted and corrected central orbit: (a) distorted central orbit; (b) corrected central orbit.

7 Discussions

The designed MEBT is based on a chopper. To control well the emittance growth is very difficult and critical while take matching and chopping the beam. Additional components including the quadru-

ples, the steering magnets, buncher, etc. serving for the chopper cause not only an increase of the cost in economy but also a longer MEBT and a larger emittance growth enhancement. In addition, it is also a challenge mechanically and technically for so many components to be installed in so narrow a space. If not using a chopper in MEBT, then the design

of MEBT becomes simple. One such way is that, MEBT consists of 4 quadrupoles and 1 buncher, and both the transversal and the longitudinal matching is fully realized by the 4 quadrupoles and the buncher. Then the length of MEBT is short and the emittance growth becomes smaller. Another alternative and more aggressive way is that DTL connects directly with RFQ without MEBT. For this way, the transversal matching between RFQ and DTL is done through adjusting the four quadrupoles installed in the first four drift tubes of DTL. Since the emittance

and beam parameters will be different at the exit of RFQ for different beam current due to the space charge force effect, simulations are being done to determine the required field adjusting range of the first four quadrupoles of DTL. Then the only remaining challenge for this way is the technical feasibility for the field adjusting range of the quadrupoles. Further study and experiment are also being done to examine whether the chopped beam quality fully satisfies the injection requirements asked by RCS through the pre-chopper.

References

- 1 FANG S X, FU S N et al. *J. of the Korean Phys. Soc.*, 2006, **48**(4): 697—702
- 2 WEI J, FANG S X et al. *J. Korean Phys.*, 2007, **50**(5): 1373—1377
- 3 Stamples J, Oshatz D et al. *Proc. of LINAC2000*. 250—252
- 4 FU S N, Kato T. *Nucl. Instrum. Methods A*, 2001, **457**: 423—437
- 5 Kurennoy S S, Power J F. *Proc. of LINAC98*. 1004—1006
- 6 FU S N, Kato T. *Nucl. Instrum. Methods A*, 2000, **440**: 296—306
- 7 Crandall K R, Rusthoi D P. *Los Alamos Report LAUR-97-886*
- 8 Ryne R (ed.). *Proc. of CAP.93. AIP Conference Proceedings 297*. 1993
- 9 LIU H C, OUYANG H F. *Chinese Physics C (HEP & NP)* 2008, **32**(4): 280—284